Anal. Chem. **2002,** *74,* 4228−4234

Volume of Pharmaceutical Powders Probed by Frequency-Domain Photon Migration Measurements of Multiply Scattered Light

Tianshu Pan and Eva M. Sevick-Muraca*

Department of Chemical Engineering, Texas A&M University, College Station, Texas 77843-3122

Using probability distribution analysis to describe the propagation of multiply scattered light between a point source and point detector located a known distance apart, mathematical expressions predicting the volume of sampled powder were determined for infinite and semi-infinite powder beds and then compared to experimental measurements of frequency-domain photon migration (FDPM). Our results show that the volume of powder sampled varies with optical properties and, when using FDPM techniques, with modulation frequency. For a typical measurement in lactose powder, the volume of powder sampled by multiply scattered light propagating between a 1000-μm-diameter point source and point detector pair separated by 8 mm is predicted to be 1.8 and 1.5 cm^3 at modulated frequencies of 50 and 100 MHz, respectively. Experimental measurements in lactose powder confirm the predictions.

Although the blending of powder and granular materials represents a crucial operation in many industries, the pharmaceutical industry continues to struggle for an economical method to validate the uniformity of active ingredients in dry powder blending operations. Although HPLC analysis can provide accurate analytical assessment for validating blend homogeneity, it nonetheless requires multiple-site, thief sampling from the powder blend. Thief sampling itself induces significant and overwhelming variance that can erroneously impact the determination of content uniformity across the entire powder bed.[1] More recently, in situ NIR reflectance spectroscopy has been proposed as a means by which content uniformity can be assessed without the need to sample by simply marking changes in the differential reflectance spectrum of the powder bed as a function of blending time.[2] NIR spectroscopy can be adapted as a method for determining blend content uniformity, either through the use of fiber optics threaded down the stationary axis of a rotating blender to a stationary spectrometer[3,4] or by affixing the entire spectrometer to a watchglass as an "on-board" analyzer. Regardless, it is desirable to assess the volume of powder analyzed for regulatory purposes. The scattering capacity of a powder determines the volume sampled by photons that propagate from a source to one or more detectors, which in the case of NIR spectroscopy, is often limited. Limited reports found in the literature show that the scattering capacity (and, hence, sampling volume) depends on the particle refractive index, particle size, packing, and diameter of NIR probe.[5−7] The mass of powder that photons sample has been reported to be 10 mg for a 4-mm NIR probe,[7] and the volume of powder that photons sample has been reported to be equivalent to that of a cylinder, the diameter of which is at least two times larger than that of the irradiated sample surface and height is approximately 1 mm.[6] In studies to systematically study the volume of powders interrogated, Cho et al.[3] related the measurement of spectral variance to the sampled volume while Berntsson et al.[5] assessed how the measurements of diffuse reflectance from a finite thickness of powder compared with that in a semi-infinite powder in order to assess the penetration depth. All studies have the common finding that the volume of powder sampled from reflectance measurements is considerably less than the current GMP that suggests sample sizes of one to three times the single dosage, which typically represents 100−1000 mg of powder mass or 0.5−5 cm^3 of uncompressed powder.

Recently, we introduced the use of time-dependent measurements of multiply scattered light as a means for assessing blend content uniformity.[8] In contrast to NIR spectroscopy measurements whereby the incident source and detector(s) are in close proximity for increased signal-to-noise ratio, measurements of multiply scattered light require that the position of incident source and light collectors are distinct and distant from one another so that the detected light has been multiply scattered and has sampled significant volumes. Time-dependent measurements assess the propagation characteristics (i.e., the photon "time-of-flight") of multiply scattered light as it samples a volume of

* To whom correspondence should be addressed. Phone: (979)-458-3206. Fax: (979)-845-6446. E-mail: sevick@che.tamu.edu.

(1) Muzzio, F. J.; Robinson, P.; Wightman, C.; Brone, D. *Int. J. Pharm.* **1997**, *155*, 153−178.
(2) Wargo, D. J.; Drennen, J. K. *J. Pharm. Biomed. Anal.* **1996**, *14*, 1415−1423.
(3) Cho, J. H.; Gemperline, P. J.; Aldridge, P. K.; Sekulic, S. S. *Anal. Chim. Acta* **1997**, *348*, 303−310.
(4) Sekulic, S. S.; Wakeman, J.; Doherty, P.; Hailey, P. A. *J. Pharm. Biomed. Anal.* **1998**, *17*, 1285−1309.
(5) Berntsson, O.; Burger, T.; Folestad, S.; Danielsson, L. D.; Kuhn, J.; Fricke, J. *Anal. Chem.* **1999**, *71*, 617−623.
(6) Moradi, K.; Depecker, C.; Barbillat, J.; Corset, J. *Spectrochim. Acta, Part A* **1999**, *55*, 43−64.
(7) Berntsson, O.; Danielsson, L. G.; Johansson, M. O.; Folestad, S. *Anal. Chim. Acta* **2000**, *419*, 45−54.
(8) Shinde, R. R.; Balgi, G. V.; Nail, S. L.; Sevick, E. M. *J. Pharm. Sci.* **1999**, *88*, 959−966.

10.1021/ac011267z CCC: $22.00
Published on Web 06/28/2002

powder. Specifically, we have focused upon one form of time-dependent measurement of multiply scattered light, frequency-domain photon migration (FDPM), which can be operated in either visible or NIR wavelength ranges, as a means for assessing content uniformity of a powder bed.

FDPM measurements consist of launching intensity-modulated light (with modulation frequencies on the order of hundreds of megahertz) and detecting the (i) average-intensity attenuation, (ii) amplitude attenuation, and (iii) phase delay at a detector point away from the incident light source between the detected and incident signals. By employing the solutions to the time-dependent optical diffusion equations,[9] the influence of light scattering and absorption on the above measured quantities provides a direct way to extract the elastic, isotropic scattering and absorption coefficients simultaneously with both high accuracy and precision.[10] By implementing FDPM using multiple wavelengths, content uniformity of multiple components in a powder sample can be obtained from direct measurements of absorption without the confounding effects of scattering. Traditional CW or intensity-based techniques suffer in this regard in that attenuation is due to the product of absorption and scattering properties, both of which are wavelength-dependent. Accurate separation of absorption and scattering spectra from intensity measurements requires a priori information of the scattering cross section and angular dependence, which is often not known in pharmaceutical systems, or a differential measurement, which may or may not effectively separate the absorption and scattering mechanisms that both attenuate light.

In this contribution, we use a general probability analysis in order to develop from the first principles the general relationship for the migration of light between a single point source and point detector in infinite and semi-infinite geometries on any powder of measured optical properties to show FDPM ability in probing powder volumes that are consistent with FDA guidance on sampling. We show that with accurate FDPM evaluation of absorption and elastic scattering properties, the volume of powder sampled by multiple scattered photons can be theoretically derived using diffusion theory to the radiative transport equation. In the limit of infinite signal-to-noise ratio (SNR), the entire available powder volume is sampled by the propagating photons. Since practical measurement limitations limit FDPM SNR, we experimentally validate theoretical predictions and identify the photon sampling volume of highest cumulative photon visitation probability that can be practically measured by using a small light-absorbing heterogeneity placed at various locations within the powder bed to measure perturbations in light propagation within the sampling volume.

THEORY

In this section, the development of the analytical expression predicting the volume of powder sampled between a point source and a point detector (or collector) is briefly described. Figure 1 provides a schematic representation of the physics behind the analytical formulation. The associated probability density for a photon, which contributes to the alternating part of an intensity-modulated wave, to originate from a modulated source at position $(-\rho, 0, 0)$ and reach a powder element located at position (x, y, z) is denoted by $\Phi_1(r_1, \omega)$, where r_1 is the distance between the source and (x, y, z) within the powder; and ω is the modulation frequency. It is well-known that the random-walk probability for finding a diffusing entity at position (x, y, z) can be obtained from the solution to the macroscale diffusion equation.[11,12] Consequently, we similarly predict the probability density Φ_1 for photon visitation with the photon density $U_1(x, y, z, \omega)$ (in photons length^{-3}), which is predicted from the optical diffusion equation and corresponding boundary conditions,

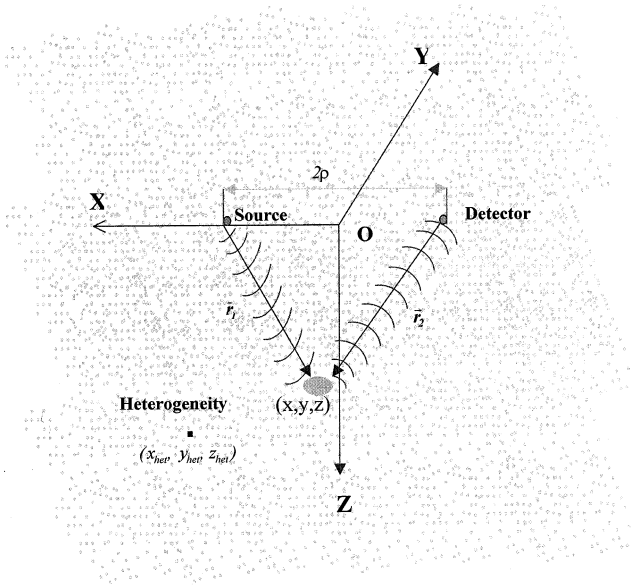

Figure 1. Schematic representation of geometry used for measurement of multiply scattering light. The origin is located on the plane containing source and detector and is located at the midpoint of the line connecting the point source at $(-\rho, 0, 0)$ and point detector at $(\rho, 0, 0)$. The position vectors $\vec{r}_1$ and $\vec{r}_2$ describe the vectors from the source to position (x, y, z) and from the detector to position (x, y, z), respectively. The absorbing heterogeneity used to assess photon densities is located at $(x_{het}, y_{het}, z_{het})$.

$$\Phi_1(r_1,\omega) = C_1^{\text{Norm}} U_1(x,y,z,\omega) \qquad (1)$$

where C_1^{Norm} is a normalization factor.

According to the reciprocality principle, the probability of an intensity-modulated wave that is emitted in the medium at position (x, y, z) and reaches detector position $(\rho, 0, 0)$ can be considered to be the same as when it is detected at position (x, y, z) following emission at position $(\rho, 0, 0)$. We similarly denote the associated probability density of an intensity modulated wave originating from position $(\rho, 0, 0)$ and traveling to an element at position (x, y, z) with $\Phi_2(r_2, \omega)$, where r_2 is the distance between the detector and location (x, y, z). Consequently, the joint probability density that a photon, which has been emitted at the modulated source and has been collected at the detector, has visited an element at

(9) Sevick, E. M.; Chance, B.; Leigh, J.; Nioka, S.; Maris, M. *Anal. Biochem.* **1991**, *195*, 330−351.
(10) Sun, Z.; Huang, Y.; Sevick, E. M. *Rev. Sci. Instrum.* **2002**, *73*, 383−393.
(11) Chandrasekhar, S. *Rev. Mod. Phys.* **1943**, *15*, 1−89.
(12) Hiemenz, P. C.; Rajagopalan, R. *Principles of Colloid and Surface Chemistry*, 3rd ed.; Marcel Dekker: New York, 1997; pp 89−97.

position (x, y, z) is given by the product of these two consecutive probability densities multiplied by a normalization factor C_2^{Norm},

$$\Phi(x,y,z,\omega) = C_2^{\text{Norm}}[\Phi_1(r_1,\omega)\Phi_2(r_2,\omega)] \quad (2)$$

The normalized probability density for photon visitation by only those photons that are ultimately detected is predicted by f_{density} at (x, y, z) (See Supporting Information).

$$f_{\text{density}}(x,y,z,\omega) = \frac{\Phi(x,y,z,\omega)}{\int_\infty \Phi(x,y,z,\omega)\, dV} \quad (3)$$

The cumulative probability that a photon has traveled within volume, V, is given by

$$P = \int_V f(x,y,z,\omega)\, dV \quad (4)$$

In the limit of a "perfect" sensor with infinitely low noise floor, $P \rightarrow 1$ as $V \rightarrow \infty$. Yet for an actual system, the noise floor is finite, and there exists a finite volume that is effectively "sampled" with probability $P < 1$.

The sampling volume can be regarded as that region visited by photons that contribute to the actual detected signal. In the "blank" region, the few number of photons that sample the blank region but ultimately reach the detector is small and below the noise floor of the detection system. In other words, photons that interrogate the blank region do not significantly contribute to the signal. A small light-absorbing volume within an otherwise homogeneous sampled volume impacts light propagation and consequently causes perturbation to the FDPM measurements. If the absorbing volume is positioned in the blank region, then to a first approximation, no perturbation in the FDPM measurements will arise, since the contributing photons are small in number. Therefore, the volume sampled by FDPM can be confirmed experimentally by assessing changes in FDPM signals upon passing a small light-absorbing heterogeneity throughout the volume of powder interrogated by signals. The "sampling" volume of FDPM measurements is defined by the cumulative probability, P, which is less than unity and which is determined by the SNR of the measurement.

In the following, we present the expressions for sampling volume for two relevant cases: (i) when the point source and point detector are located within an infinite medium and, more relevant for actual measurements, (ii) when they are positioned on the surface of a semi-infinite medium. It is also noteworthy that since we derive our formulations generally, the analytical expressions are applicable to CW or intensity-based measurements ($\omega = 0$), as well as any homogeneous medium (on length scale of an isotropic scattering length) that multiply scatters light.

Sampled Volume in an Infinite Medium. The solution to the optical diffusion equation within an infinite medium provides the distribution of photon density[13] and, hence, corresponding probability density, as shown in eq 1,

$$\Phi_1(r_1,\omega) = C_1^{\text{Norm}} \frac{SA}{4\pi D c r_1} \times \left|\exp\left(-\sqrt{\frac{m}{Dc}} r_1 e^{\theta i/2}\right)\right| \quad (5)$$

where

$$m = \sqrt{(\mu_a c)^2 + \omega^2}$$

$$\theta = \tan^{-1}\left(\frac{\omega}{\mu_a c}\right)$$

$$D = \frac{1}{3(\mu_a + \mu_s')}$$

Here, c is the speed of light; μ_a is the absorption coefficient; μ_s' is the isotropic scattering coefficient; S is the fluence of the source (photons per second), and A is the modulation depth of the source. As described earlier, $\Phi_2(r_2, \omega)$ is derived through the use of the reciprocality principle, and the joint probability density for photon visitation from the source to an element at position (x, y, z) and to the detector can be computed from eq 2.

It should be noted that although the application of the diffusion model holds strictly for multiply scattered light (whereby $\mu_a \ll \mu_s'$), the use of Monte Carlo and radiative transfer equation is appropriate when the diffusion approximation may not hold. For powders, the use of the diffusion approximation to the radiative transfer equation provides an efficient computation and analytical solution and is typically correct for the visible wavelength range for pharmaceutically relevant compounds.

To obtain an analytical resolution of sampled volume, the Cartesian system is transformed into a prolate spherical coordinate system[14] in which

$$x = \rho \cosh \xi \cos \eta, \quad y = \rho \sinh \xi \sin \eta \sin \phi, \quad z = \rho \sinh \xi \sin \eta \cos \phi \quad (6)$$

$$(0 \le \xi \le \infty, \quad 0 \le \eta \le \pi, \quad \text{and } 0 \le \phi \le 2\pi)$$

and the normalized probability, P, that a photon has traveled in prolate volume of radius ξ can be determined from eq 4 (see Supporting Information),

$$P = 1 - e^{-2h(\cos\xi - 1)} \quad (7)$$

where we define h as a dimensionless parameter that is given by

$$h = \sqrt{\frac{m}{Dc}} \rho \cos\frac{\theta}{2}$$

The volume of a region to be visited by sampling photons with a probability P can be explicitly derived (see Supporting Information).

(13) Fishkin, J.; Gratton, E. *J. Opt. Soc. Am. A* **1993**, *10*, 127−140.

(14) Happel, J.; Brenner, H. *Low Reynolds Number Hydrodynamics, with Special Applications to Particulate Media*; Prentice-Hall: Englewood Cliffs, NJ 1965; Appendix A

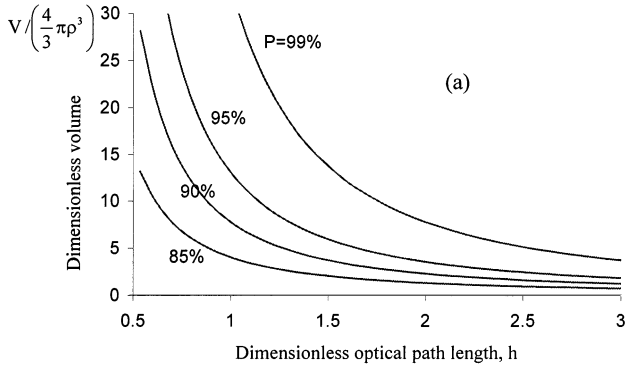

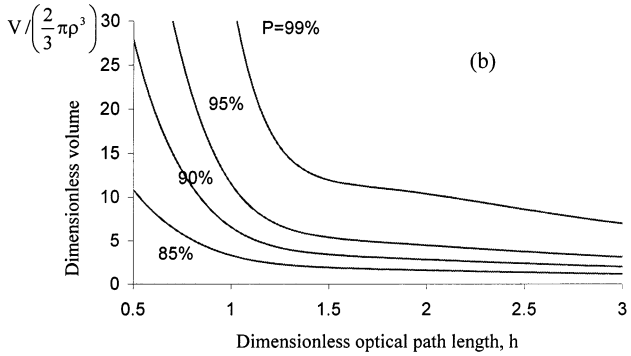

$$h = \sqrt{\frac{m}{Dc}}\rho\cos\frac{\theta}{2}$$

Figure 2. The dimensionless volume for infinite (a) and semi-infinite media (b) as a function of dimensionless parameter *h* for various probabilities, *P*, associated with detection limits.

$$V(P) = \frac{4}{3}\pi\rho^3\left[\left(1 + \frac{1}{2h}\ln\frac{1}{1-P}\right)^3 - \left(1 + \frac{1}{2h}\ln\frac{1}{1-P}\right)\right] \quad (8)$$

From eq 8 one can see that the volume interrogated at a cumulative probability, *P*, is proportional to ρ^3 and depends on the parameter *h*. Physically, parameter *h* represents, in the case of nonabsorbing medium, the ratio of the distance between the incident and detector fibers to the wavelength of the propagated photon density wave.[13]

Although the volume of powder sampled by all photons ($P = 1$) is ideally infinite, the measurement SNR limits the volume actually interrogated to that associated with a probability that is <1. Figure 2a lists the dimensionless volume interrogated by a point source and point detector within an infinite medium as a function of dimensionless parameter *h*. As described below, the maximum cumulative probability associated with volumes interrogated ranged between $P = 0.90$ and $P = 0.99$.

Sampled Volume in Semi-Infinite Medium. Similarly, the normalized probabilities for the semi-infinite medium can also be obtained from the approximate solution to the diffusion equation employing zero-boundary conditions.[15] The sampled volume at cumulative probability *P* can be likewise derived,

$$V(P) = \frac{2}{3}\pi\rho^3(\cosh^3\xi_{(P)} - \cosh\xi_{(P)}) \quad (9)$$

where the dimensional prolate spheroidal volume, $V(P)$, is defined by the radius corresponding to cumulative probability, *P*, and $\xi_{(P)}$ is therefore implicitly a function of the cumulative probability, *P*. The explicit relationship defining the cumulative probability at prolate spheroidal radius ξ, is given by

$$P(\xi) = \frac{F(\xi)}{F(\infty)}$$

$$F(\xi) = \sum_{i=1}^{5} b_i E(\xi,h,i-3) + \sum_{i=1}^{5}\sum_{j=1}^{4} e_i p_j (E(\xi,h,i+j-4) + d_1 E(\xi,h+d_2,i+j-4)) \quad (10)$$

where *E* is an exponential integral defined along with other parameters in the Supporting Information.

Figure 2b illustrates the dimensionless volume interrogated as a function of probability and dimensionless optical path length for semi-infinite media.

METHODS AND MATERIALS

To evaluate the volume interrogated by multiply scattered light and determine the cumulative probability limits for photon sampling, FDPM measurements were conducted on dry monohydrate lactose powder [SIGMA, St. Louis, MO]. The instrumentation associated with FDPM measurements is described elsewhere.[8] Briefly, 25 mW intensity-modulated 687-nm light from a laser diode (model TCLDM9, Thorlabs, Newton, NJ) was directed into a 1.5 m, 1000 μm (diameter) fiber (model FT-035 mm, Thorlabs, Newton, NJ), the free end of which was positioned within the scattering sample. Intensity modulation of the laser diode was accomplished by imposing a 13 dB RF signal under frequencies at 50 and 100 MHz using a bias tee. Similarly, a second 1.7 m, 1000-μm detector fiber was positioned within the powder with its free end at the same horizontal level (z) as the incident fiber (see Figure 1). The modulated light collected by the fiber was directed to a photomultiplier tube (PMT) (model H6357, Hamamatsu, Japan) modulated at the same frequency as the laser diode, but with a 100 kHz offset frequency. The mixed PMT signal was then passed through a transimpedance amplifier that removed high-frequency components and enabled collection by LabView data acquisition software (National Instrument). Measurements of average intensity (DC), amplitude intensity (AC), and phase shift (PS) were recorded. Although our measurements were performed at 687 nm, the results should be analogous at other energies.

The optical properties of the powder were determined by conducting FDPM measurements from 50 to 100 MHz as the distance between the source and detector fibers was varied between 4 and 8 mm, accurately accomplished by a programmable motion controller (model PMC 200-P, Newport, Irvine, CA). The values of DC and PS as a function of source/detector fibers were fit to the solution of the optical diffusion equations to provide values of μ_a and μ_s'.[10] Herein, the obtained optical properties of the lactose were found to be $\mu_a = 0.0144 \pm 0.0006$ cm^{-1} and $\mu_s' = (2.5 \pm 0.1) \times 10^2$ cm^{-1} at $\lambda = 687$ nm.

Testing Sampled Volume Using an Absorbing Heterogeneity. To probe the volume sampled by propagating photons

(15) Haskell, R. C.; Svaasand, L. O.; Tsay, T.; Feng, T.; McAdams, M. S.; Tromberg, B. J. *J. Opt. Soc. Am. A* **1994**, *11*, 2727−2741.

within the lactose powder bed, FDPM measurements were conducted between source and detector fibers separated by 8 mm and positioned within the powder bed containing a black, light absorbing heterogeneity. The lactose powder was held within a 50-mm-deep and 70-mm-diameter cylindrical container, inside which the two fibers could be moved in the z direction while keeping both free ends in the same $x-y$ plane.

In the absence of the heterogeneity, 20 measurements of wave amplitude (AC) at various positions along the z axis possessed a relative standard deviation of 1.5% at 50 MHz and 2.0% at 100 MHz within the homogeneous powder bed.

An 0.8-mm-diameter black plastic ball was employed as the absorbing heterogeneity used to probe the powder volume. Attached to the end of a fiber optic, the absorbing heterogeneity was positioned at a stationary point within the 50-mm-deep homogeneous powder bed 25 mm away from the top powder surface, 25 mm away from the bottom of the container, and 35 mm away from the sides of the container. The position of heterogeneity with respect to the fibers was changed by systematically retracting and inserting the fibers along the z axis at various $x-y$ planes surrounding the heterogeneity. When AC measurements indicated a value change exceeding 1.5% at 50 MHz or 2.0% at 100 MHz of that for the homogeneous case, heterogeneity was assumed to reside in the sampled volume. Likewise, if the change of AC measurement was within 1.5% at 50 MHz or 2.0% at 100 MHz of that for homogeneous case, then the absorbing heterogeneity was assumed to be positioned in the blank region.

To a first approximation, the perturbation caused by the small absorbing heterogeneity is correlated to the probability density. The perturbation owing to the absorbing heterogeneity is represented as the $\ln[(AC)_\infty/(AC)_{het}]$ and is approximately proportional to the probability density associated with the volume of heterogeneity, ΔV^{het}

$$\ln[(AC)_\infty/(AC)_{het}] \propto \int_{\Delta V^{het}} f_{density}\, dV \qquad (11)$$

where $(AC)_\infty$and $(AC)_{het}$ refer to the AC values in the absence and presence of heterogeneity, respectively. The probability density, $f_{density}$, is calculated from eq 3 for an infinite medium.

RESULTS AND DISCUSSION

Figure 3 plots the comparison between the measured AC values (symbols) and those calculated by eq 11 (dashed line) at 50 MHz as the position of heterogeneity (2 mm, 0 mm, z_{het}) varies along the z axis. Although the values of the perturbed measurements and their predictions may not be expected to agree owing to finite size of the absorbing heterogeneity (and especially when close to the source and detector), the comparable trends nonetheless show that at positions distant from the source and detector, the absorbing heterogeneity impacts FDPM measurements in a manner consistent with the probability density predicted by eq 11.

Figure 4a shows the measured AC values at 50 MHz as a function z position of the heterogeneity at differing x positions within the powder bed. The reduction in the AC value occurs as a result of absorption of photons and provides an assessment of the probability density at the position (x, 0, z) associated with the heterogeneity. Figure 4b represents the contour map of the

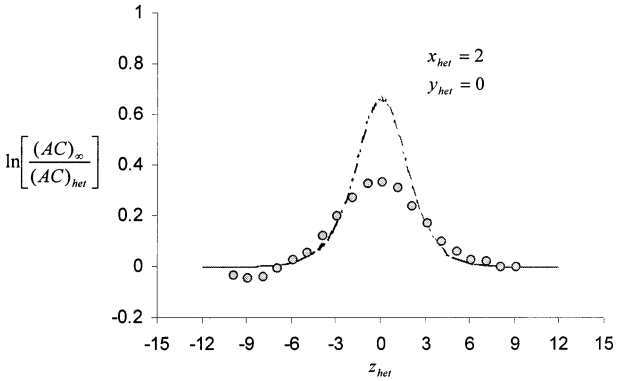

Figure 3. Comparison of experimental and theoretical values of amplitude attenuation as a function of z [mm] position of the absorbing heterogeneity located at (x_{het}, y_{het}, z_{het}) = (2 mm, 0, z_{het}). The separation between the source and detector is 8 mm and ω = 50 MHz. The dashed line denotes theoretical values as calculated by eq 11, and the solid points are experimental values.

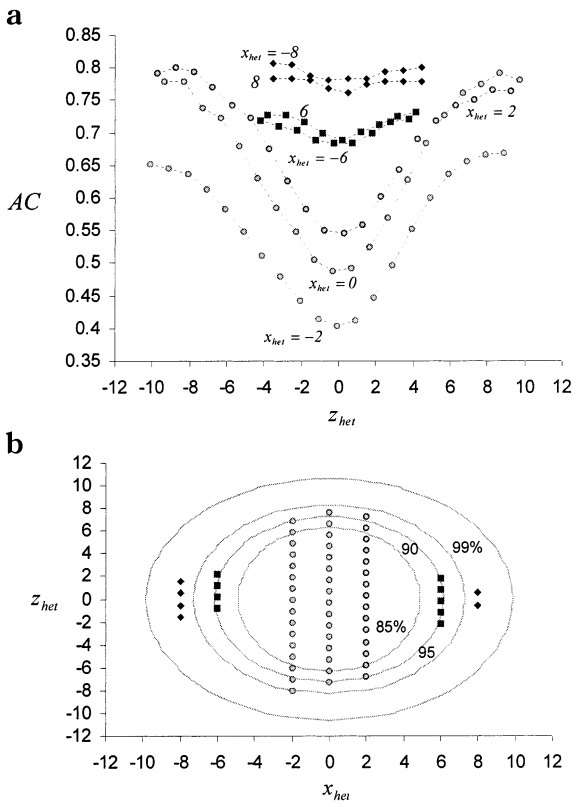

Figure 4. (a) Values of AC attenuation measured at ω = 50 MHz in the presence of absorbing heterogeneity located at (x_{het}, 0, z_{het}) and as a function of z_{het} [mm] for various x_{het} [mm]. (b) Contour map of P in the x [mm]$-z$ [mm] plane at y = 0 mm (solid lines predicted from eq 7) and as interrogated by the absorbing heterogeneity and AC measurements at ω = 50 MHz. The symbols denote heterogeneity locations (x_{het}, 0, z_{het}). where perturbation in AC measurements exceeded 1.5%. The symbols denote the level of perturbation: the filled circles denote a 1.5−38% perturbation level; the filled squares, 1.5−5.4% perturbation level; and the filled diamonds, 1.5−3.0% perturbation level.

associated cumulative probabilities, P, in the $x-z$ plane, and the symbols denote heterogeneity locations (x_{het}, 0, z_{het}) where the change in AC measurement exceeded 1.5% of the mean AC measured in the homogeneous case. The symbols denote the level of AC perturbation from the homogeneous case in which the filled

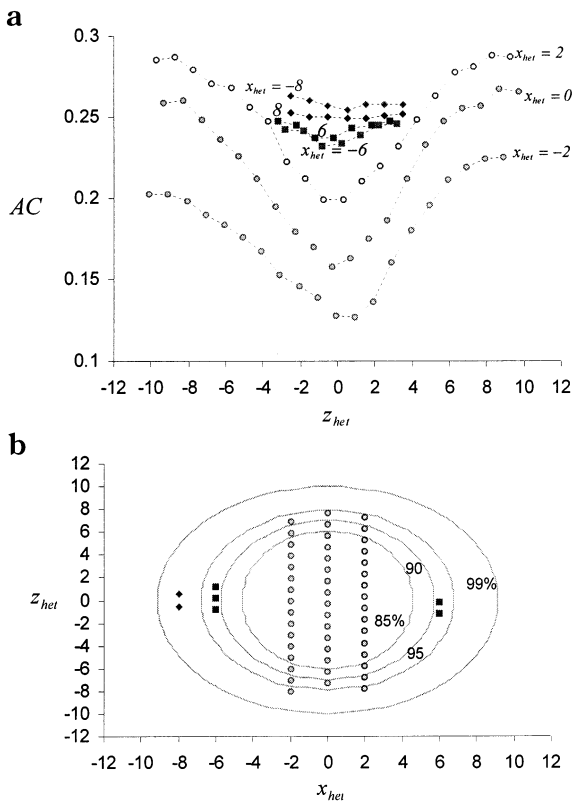

Figure 5. (a) Values of AC attenuation measured at $\omega = 100$ MHz in the presence of absorbing heterogeneity located at (x_{het}, 0, z_{het}) and as a function of z_{het} [mm] for various x_{het} [mm]. (b) Contour map of P in the x [mm]−z [mm] plane at $y = 0$ mm (solid lines predicted from eq 7) and as interrogated by the absorbing heterogeneity and AC measurements at $\omega = 100$ MHz. The symbols denote heterogeneity locations (x_{het}, 0, z_{het}) where perturbation in AC measurements exceeded 2.0%. The symbols denote the level of perturbation: the filled circles denote a 2.0−39% perturbation level; the filled squares, 2.0−5.7% perturbation level; and the filled diamonds, 2.0−3.4% perturbation level.

circles denote regions associated up to a 38% change; the filled squares, up to a 5.4% change; and the filled diamonds, up to a 3.0% change. Clearly, the smallest perturbation in AC measurements occurs farthest from the source−detector pair where the cumulative probability for visitation is the highest. Inspection of Figure 4b indicates that the locations (x_{het}, 0, z_{het}) that result in detectable AC perturbation reside in the areas where P is predicted to be ≤95% probability region (see Supporting Information). No significant perturbation was recorded once the heterogeneity was positioned outside this region. In other words, a variation of optical properties in those volumes other than the present 95% probability region is unlikely to cause a change in the received signals by the FDPM employed and is, thus, unlikely to be detected. Therefore, the sampled volume is limited under the present SNR of our FDPM instrument to the 95% probability region.

Figure 5a likewise shows the measured AC values at 100 MHz as a function z position of the heterogeneity at differing x positions within the powder bed. Figure 5b represents the contour map of the cumulative probability, P, in the x−z plane, and the symbols denote heterogeneity locations (x_{het}, 0, z_{het}) where AC perturbations from the homogeneous case exceeded 2.0%. The symbols denote the level of AC perturbation from the homogeneous case in which the filled circles denote regions associated with 2.0−39% change; the filled squares, 2.0−5.7% change; and the filled diamonds, 2.0−3.4% change. Inspection of Figure 5b also indicates that the locations (x_{het}, 0, z_{het}) that result in detectable AC perturbations reside in the areas where P is predicted to be ≤95% probability region, consistent with the results obtained at 50 MHz.

Increasing modulation frequency has an effect similar to the absorption coefficient μ_a on the wavelength of photon density wave: increased absorption or modulation frequency shortens the wavelength of the propagating photon density wave. Consequently, h increases from 1.39 to 1.54 when the frequency is doubled from 50 to 100 MHz, and the sampled volume predicted from eq 8 decreases from 1.8 to 1.5 cm^3 for the visiting probability of 95% in the lactose system. The volumes at the limit of experimental detection were limited to 1.5 ± 0.3 and 1.4 ± 0.2 cm^3 in terms of numerical integration over the experimental points, with detectable perturbations shown in Figures 4b and 5b. Although the use of an absorbing heterogeneity is inarguably a first-order approximation, to understand the experimental limits of sampling volume, it nonetheless enables a qualitative, if not quantitative, comparison with the theoretical predictions.

The source−detector separation, 2ρ, also impacts the volume sampled by migrating photons. On one hand, an increase in the separation distance between two fibers leads to a larger volume for migrating photons and tends to increase the sampled volume. On the other hand, an increase in separation distance weakens the received intensity and may result in a reduced signal, which may tend to offset the enlarged sampled volume if the strength of the incident source is not adjusted for compensation. Therefore, an optimal source-detector separation, 2ρ, exists that is dependent upon the SNR of the measurement. In our experience with pharmaceutically relevant powders, we find the optimal separation to be 8 mm and no greater than 1 cm.

CONCLUSIONS

An analytical model for the prediction of powder volume sampled by FDPM measurements is developed for infinite and semi-infinite media and tested in the case of infinite geometries on lactose powder. The sampled volume is determined by two parameters: (i) the separation distance between incident point source and point detector and (ii) the dimensionless parameter h, which is the ratio of the separation to the wavelength of the propagating intensity wave. Experiments of a small, light absorbing heterogeneity verify the theoretical prediction of the distribution of probability density and sampled volume. The sampled volume by FDPM in these typical experiments reaches 1.5 to 1.8 cm^3 and satisfies the FDA regulations in pharmaceutical industry. Although the prediction of sampling volume is presented herein for the case of FDPM measurements for assessing blend homogeneity, the results are translatable for CW measurements (at $\omega = 0$) and for other spectroscopy applications that involve multiple scattering, such as tissues, colloids, and other random media.

Abbreviations: AC, wave amplitude; CW, continuous wave; FDA, Food & Drug Administration; FDPM, frequency-domain photon migration; GMP, good manufacturing practice; SNR, signal-to-noise ratio.

SUPPORTING INFORMATION AVAILABLE

Supporting Information Available: Derivation of eq 3 for predicting density, derivation of eq 7 for predicting cumulative

probability, derivation of eq 8 for predicting volume, and derivation of eq 10 for a semi-infinite medium. This material is available free of charge via the Internet at http://pubs.acs.org.

Received for review December 18, 2001. Accepted May 13, 2002.

AC011267Z